Quantitative in vivo imaging of the effects of inhibiting integrin signaling via Src and FAK on cancer cell movement

Published in final edited form as:
Cancer Res. 2010 November 15; 70(22): 9413–9422. doi:10.1158/0008-5472.CAN-10-1454.

Quantitative in vivo imaging of the effects of inhibiting integrin signalling via Src and FAK on cancer cell movement; effects on E-cadherin dynamics

Marta Canel[a], **Alan Serrels**[a], **Derek Miller**[b], **Paul Timpson**[b], **Bryan Serrels**[a], **Margaret C. Frame**[a], and **Valerie G. Brunton**[a,1]

[a]Edinburgh Cancer Research Centre, Institute of Genetics and Molecular Medicine, University of Edinburgh, UK, EH4 2XR

[b]Beatson Institute for Cancer Research, Glasgow, UK, G61 1BD

Abstract

Most cancer related deaths are due to the development of metastatic disease and several new molecularly targeted agents in clinical development have the potential to prevent disease progression. However, it remains difficult to assess the efficacy of anti-metastatic agents in the clinical setting and an increased understanding of how such agents work at different stages of the metastatic cascade is important in guiding their clinical use. We have used optical window chambers combined with the use of photobleaching, photoactivation, and photoswitching to quantitatively measure a) tumor cell movement and proliferation by tracking small groups of cells in the context of the whole tumor, and b) E-cadherin molecular dynamics *in vivo* following perturbation of integrin signaling by inhibiting focal adhesion kinase (FAK) and Src. We show that inhibition of Src and FAK suppresses E-cadherin dependent collective cell movement in a complex 3D tumor environment, and modulate cell-cell adhesion strength and endocytosis *in vitro*. This demonstrates a novel role for integrin signaling in the regulation of E-cadherin internalization, which is linked to regulation of collective cancer cell movement. This work highlights the power of fluorescent, direct, *in vivo* imaging approaches in the pre-clinical evaluation of chemotherapeutic agents, and shows that inhibition of the Src/FAK signaling axis may provide a strategy to prevent tumor cell spread by de-regulating E-cadherin-mediated cell-cell adhesions.

Keywords

Src; FAK; collective movement; photoswitching; E-cadherin

Introduction

In their physiological environment, cells are in contact with surrounding extracellular matrix (ECM) and with neighbouring cells. While cell–matrix adhesions are largely integrin-based, cell–cell junctions are mediated by AJs, tight junctions and desmosomes. Cadherin-based AJs provide the initial means of cell–cell contact and have key roles during development and maintenance of epithelial polarity (1, 2). Additionally, there is overwhelming evidence that E-cadherin is an important tumor and/or invasion suppressor (3-5). Tumor cells employ a number of strategies to move *in vivo*; either as individual cells or collectively as cohesive

[1]Correspondence: Valerie Brunton, Edinburgh Cancer Research Centre Edinburgh University Crewe Road South Edinburgh, EH4 2XR, UK Telephone: ++ 44 131 777 3556 Fax: ++ 44 131 777 3520 v.brunton@ed.ac.uk.

Europe PMC Funders Author Manuscripts

groups of cells which maintain cell-cell contacts (6). However, many tumors can adapt their mode of movement in response to external stimuli and several lines of evidence support the idea of cross-talk between integrin-mediated cell-ECM interactions and E-cadherin-mediated cell-cell junctions which may be key to the plasticity observed in tumor cells (7, 8). Although the mechanisms involved are not understood integrin-dependent modulation of Rho GTPases and the actomyosin cytoskeleton which is tethered at both adhesion types, may play an important role (9). In addition, Src and focal adhesion kinase (FAK), two non-receptor tyrosine kinases, which are key regulators of integrin dependent matrix adhesions, have been linked to the control of AJs. Upon integrin engagement both FAK and Src tyrosine kinases are autophosphorylated on specific tyrosine residues at integrin-mediated adhesions. FAK autophosphorylation on Y397 creates a high affinity binding site for the SH2 domain of Src which leads to the Src-dependent phosphorylation of FAK on additional tyrosine residues. These act as protein-protein interaction motifs and link the FAK-Src complex to a number of downstream signaling pathways (10). Increased Src activity is associated with the disruption of E-cadherin dependent AJs and this was shown to be dependent on integrin signalling and FAK phosphorylation indicating that the Src/FAK signalling axis may play an important role in the cross-talk between integrin- and E-cadherin-dependent adhesions (7).

Most cancer related deaths are due to the development of metastatic disease and several new molecularly targeted agents in clinical development (including those targeting both Src and FAK) have the potential to prevent disease progression (11). However, it remains difficult to assess the efficacy of anti-metastatic agents in the clinical setting and an increased understanding of how such agents work at different stages of the metastatic cascade is important in guiding their clinical use. As the tumor microenvironment plays a key role in disease progression (12) it is becoming evident that the use of appropriate animal models is essential for determining the activity of such agents. In order for cells to metastasize to distant sites they must undergo a number of phenotypic changes including changes in cell-matrix and cell-cell adhesions, migration and invasive capacity but these have been difficult to monitor *in vivo*. Here we describe the use of optical window chambers in combination with photobleaching, photoactivation and photoswitching to quantitatively measure collective tumor cell movement, proliferation and protein dynamics in squamous cell carcinoma cells within a tumor mass *in vivo*. We demonstrate that inhibiting the Src/FAK signaling axis prevents the collective movement of tumor cells *in vitro* and *in vivo*, and identify a novel role for this pathway in the regulation of E-cadherin internalization, cell-cell adhesion strength, and modulation of E-cadherin dynamics downstream of β1-integrin. Taken together this data highlights the benefits of fluorescent *in vivo* imaging approaches together with the use of optical window chambers in the pre-clinical evaluation of potential chemotherapeutic agents, and suggests that the anti-invasive properties of small molecular inhibitors targeting Src and FAK may be mediated in part by their ability to regulate cell-cell adhesion.

Materials and Methods

Cell culture

A431 cells (LGC Promochem) were transfected with GFP-E-cadherin (13), pDendra2 (Evrogen), nuclear photoactivatable Green Cherry (nG^{PA}C) (14) or Y527F Src-GFP (15) using the Amaxa nucleofector transfection system (Amaxa GmbH). Cells stably expressing siRNA against β1-integrin and their corresponding control cells were a kind gift from Erik Sahai (16). For siRNA experiments cells were transfected with 50 nM of E-cadherin or FAK siRNA smartpool or siCONTROL pool1 (Dharmacon) using the Amaxa nucleofector transfection system. The following treatments were used: β1 blocking Ab, clone mAb13

(17) 2 μg/ml, 1 - 3 h; dynasore (Sigma) 80 μM, 0.5 - 2 h; PF-562,271 (Pfizer), 250 nM, 1 - 72 h; dasatinib (Bristol Myers Squibb) 200 nM, 1 – 72 h.

Collagen invasion assays

Cells were seeded on the bottom of transwell inserts (Corning) containing rat tail collagen type I (Roche). Transwell inserts were then placed in serum-free medium, and medium supplemented with 10% FCS and 10 ng/ml EGF was placed on top of the gel. After 5 days, cells were stained with Calcein AM (Molecular Probes). Horizontal z-sections through the gel were taken at 10 μm intervals using an Olympus FV1000 confocal microscope. The number of positive pixels in each image was determined using 'Image J' software (NIH). The values obtained for individual sections were normalized over the sum of values for all the sections and then expressed as a percentage of the control cell value. For each experiment, samples were run in triplicate and at least four z-series were taken per sample. Projected images used for display purposes were also created using 'Image J'.

Dispase-based dissociation assay

Quantification of adhesion strength following mechanical stress of dispase treated monolayers was determined as previously described (18).

Surgical Implantation of Optical Window Chambers

Optical window chambers were implanted into CD-1 nude mice under anaesthesia. All animal work was carried out in compliance with UK Home Office guidelines. Optical window chambers were custom fabricated using aluminum (19). To install the window dorsal skin was sutured to a c-clamp template. A circle of skin was removed and screw holes made using a 2 mm biopsy punch. The frame of the window chamber was then fitted to either side of the skin-flap and secured using screwing nuts; the tightness of which was adjusted to ensure that blood vessels were not occluded. The window was then sutured to the skin and the c-clamp removed. A small piece of tumor was placed into the centre of the window and sealed with a coverslip. Tumors were allowed to establish under the windows for 10 days prior to imaging at which time there was extensive re-vascularization (Figure S1A,B, Movie S1). Further details on the optical window chambers are provided in Supplementary Methods.

Immunoblot analysis

Immunoblot analysis was performed as previously described (20). Primary antibodies used were anti-GFP (Abcam), anti-E-cadherin, anti-FAK (Becton Dickinson Transduction Laboratories), anti-pY397 FAK, anti-pY861 FAK (Biosource), anti-pY416 Src, anti-Src (Cell Signaling), β1-integrin (Chemicon) and anti-γ-tubulin (Sigma) all at 1:1000 dilution.

FRAP analysis

For *in vitro* measurements cells were maintained at 37°C in a temperature controlled chamber while animals were maintained at 37°C on a heated stage for *in vivo* measurements. Experiments were performed using an Olympus FV1000 confocal microscope with SIM scanner. For photobleaching the following settings were used: pixel dwell time 4 μs/px, pixel resolution 512 × 512, 5% 488 nm laser power (30% for *in vivo*) 488 nm laser power, pinhole 250 μm, 60x Oil 1.35 N.A. objective (40× water 0.8 N.A. for *in vivo*), and a 3× zoom. Effective photobleaching was achieved using 50% (40% for *in vivo*) 405 nm laser power, 20 μs/pixel (40 μs/pixel for *in vivo*) dwell time, and a 1 frame (3 frames for *in vivo*) bleach time. Images were captured every 5 sec for 75 frames (100 frames for *in vivo*). For *in vitro* experiments, approximately 25 cells were imaged over 3 independent experiments, and for *in vivo* experiments 5 animals were imaged per condition

with 6 movies captured from each animal. Mice were treated with PF-562,271 (33 mg/kg in 0.5% methylcellulose, p.o. by gavage) 30 minutes prior to imaging. Fluorescent intensity measurements derived from the region of interest used to bleach were averaged in Excel and used to plot recovery / decay curves. Average measurements for each time-point were exported into SigmaPlot (Systat Inc) for exponential curve fitting. The half-time of recovery ($t_{1/2}$) was calculated as described previously (21).

In vivo photoswitching

Dendra2 expressing tumors were implanted in optical window chambers and imaged at 0, 6 and 24 hours after photoswitching. All images were captured using an Olympus FV1000 confocal microscope equipped with a UMPLFLN 20× 0.5 N.A. water immersion objective. Photo-switching of Dendra2 was achieved using the following settings: pixel dwell time 40 μs/px, 28% 405 nm laser power, 5 frame switching time. Mice were treated with PF-562,271 (33 mg/kg in 0.5% methylcellulose, p.o. by gavage BID) or dasatinib (15 mg/kg in 80 mM citrate buffer, p.o. by gavage qd) starting on the day of photoswitching. After photoswitching a region of interest, a z-series was acquired (sections every 10 μm) for both green and red channels. Image analysis was performed using ImageJ. Each z-series was flattened into one image using the maximum z-intensity projection tool, thresholded, and the area occupied by the red fluorescent channel measured. This area was plotted over time as a fold increase in area occupied by migrating cells.

Endocytosis of E-cadherin

Quantification of biotinylated E-cadherin endocytosis was performed as described previously (18).

Further experimental details are given in S1 Text.

Results

FAK and Src regulate A431 collective cell movement *in vitro* and *in vivo*

We have previously demonstrated that A431 cells invade in a collective manner *in vitro* which is dependent on the presence of E-cadherin dependent AJs (20). Treatment of cells with either the FAK inhibitor PF-562,271 or the Src inhibitor dasatinib resulted in complete inhibition of collective cell invasion into collagen (Figure 1A), at a concentration where FAK kinase activity (as measured by FAK autophosphorylation on Y397) and Src activity (as measured by Src autophosphorylation at Y416) were inhibited respectively (Figure 1B). Treatment of cells with dasatinib also inhibited the Src-dependent phosphorylation of FAK on Y861 (Figure 1B). To enable imaging and quantification of tumor cell movement *in vivo*, cells were transfected with the photoswitchable probe Dendra2 and tumors established under observation windows (Figure S1A)(22). A subpopulation of tumor cells were marked by switching Dendra2 from its green to red emitting state and z-sections acquired over 24 hours (Figure 1C) and cell movement quantified by calculation of the fold increase in area of the red fluorescence (Figure 1D). There was extensive movement of the tumor cells over 24 hours in the vehicle treated animals which was inhibited in both dasatinib and PF-562,271 treated animals (Figure 1C, D). Similar studies were carried out in cells at the edge of the tumors. Although A431 Dendra2 cells dispersed over time we rarely detected any cells moving away from the original tumor area into the surrounding stroma within the time frame of our experiments (Figure S2) and could therefore not use this approach to follow the invasion of the A431 cells into the surrounding stroma.

While observation of A431 cell behavior *in vivo* indicated extensive cell movement, our results did not rule out the possible contribution of increased cell proliferation/survival to the

fold increase in area being measured. To address the contribution of proliferation and/or survival, A431 cells were transfected with a nuclear targeted photoactivatable GFP fused to mCherry ($nG^{PA}C$) (14). A subpopulation of tumor cells were marked by activation of the nuclear targeted photoactivatable GFP and a confocal z-series acquired over 24 hours (Figure S3A). 3-dimensional rendering and spot detection of photoactivatable GFP marked nuclei (Figure S3B) was used to quantify the number of nuclei at each time point, and calculate the fold change in nuclear number (Figure S3C). There was a 1.2 fold increase in nuclear number over 24 hours, which was unchanged following PF-562,271 treatment. This increase in nuclear number was used to normalize measurements from Figure 1D (Figure S3D). Thus FAK kinase activity does not contribute to the proliferation/survival of A431 cells *in vivo* in the time scale of this experiment, and furthermore the basal level of tumor cell proliferation was not sufficient to account for the fold increase in area measured following photoswitching.

E-cadherin modulates collective movement of A431 cells *in vitro* and *in vivo*

We have previously reported that loss of E-cadherin at sites of cell-cell adhesion inhibits collective invasion of A431 cells *in vitro* (20). However, over-expression of E-cadherin (2.3 fold increase, Figure S4A) also inhibited invasion of A431 cells into collagen (Figure 2A), suggesting that a balance exists between E-cadherin expression and collective invasive capacity. To address whether E-cadherin over-expression affected tumor cell movement *in vivo*, cells were labeled with Dendra2 and tumors established under observation windows. In contrast to control tumors, cells over-expressing E-cadherin exhibited a marked reduction in motility (Figure 2B, C). Furthermore, visual observation of acquired images revealed that A431 cells maintain their collective mode of migration *in vivo* (Figure 2D, (*) indicates individual cells within groups), suggesting that these cells are also dependent on E-cadherin mediated cell-cell adhesions for their movement *in vivo*.

FAK signaling regulates E-cadherin dynamics *in vitro and in vivo*

We have recently demonstrated that the use of fluorescence recovery after photobleaching (FRAP) allows us to monitor E-cadherin dynamics both *in vitro* and *in vivo* (21). Changes in the recovery rate of E-cadherin molecules are associated with increased migratory potential of cells. For example the recovery rate of GFP-E-cadherin following photobleaching in migrating cells is slower than in stationary cells, while inhibition of Src signaling, which reduces cell migration increases the recovery rate of GFP-E-cadherin (21). Here we set out to determine whether changes in E-cadherin dynamics were also seen following inhibition of FAK kinase activity. GFP-E-cadherin at sites of cell-cell adhesion was subjected to photobleaching (Figure 3A, Movie S2 and S3). Recovery kinetics data for GFP-E-cadherin ± PF-562,271 treatment was pooled and fitted to single exponential rise-to-maximum curves (Figure S5A). R^2 values reflected the tight fit of our data to the predicted values (Control/PF-562,271, $R^2 = 0.98$). Treatment of cells with PF-562,271 decreased the half-time of recovery ($t_{1/2}$) by 40%. To confirm these effects were specific to inhibition of FAK kinase activity we also used siRNA to knock-down FAK expression (Fig. S4B). A similar reduction in $t_{1/2}$ was seen in FAK knock-down cells (Figure 3B). As FAK is an important downstream effector of integrin signaling we carried out FRAP of GFP-E-cadherin in cells expressing β1-integrin siRNA in which there was a specific knock-down of β1-integrin protein expression (Figure S4C) and also saw a reduction in the $t_{1/2}$ (Figure 3B). These results identify β1-integrin and its downstream effector FAK as key regulators of E-cadherin dynamics and that inhibition of E-cadherin dependent collective movement correlates with an increased rate of recovery of GFP-E-cadherin.

We next asked whether changes in E-cadherin dynamics could also be used as a read-out of E-cadherin function *in vivo*. Tumors expressing GFP-E-cadherin were established under

observation windows and GFP-E-cadherin at sites of cell-cell adhesion subjected to photobleaching (Figure 3C, Movie S4 and S5). Recovery kinetics data for GFP-E-cadherin in either vehicle or PF-562,271 treated animals was pooled and fitted to single exponential rise-to-maximum curves (Figure S5B). R^2 values reflected the tight fit of our data to the predicted values (Control/ PF-562,271, $R^2 = 0.97$). Treatment of animals with PF-562,271 prior to photobleaching of GFP-E-cadherin resulted in a marked reduction in the $t_{1/2}$ (Control, 38.3 ± 3.2 seconds; PF-562,271, 20.4 ± 2.5 seconds; Figure 3D); similar to that observed *in vitro*. Thus inhibition of FAK kinase activity following treatment with PF-562,271 results in altered E-cadherin dynamics *in vivo*, which correlates with reduced E-cadherin-dependent collective cell movement.

FAK controls E-cadherin internalization and cell-cell adhesion strength downstream of β1-integrin

The observation that E-cadherin over-expression and inhibition of Src/FAK signaling both resulted in inhibition of invasion and the ability of Src/FAK to regulate E-cadherin dynamics both *in vitro* and *in vivo*, led us to hypothesize that inhibiting the Src/FAK signaling axis may regulate the collective movement of A431 cells via regulation of E-cadherin. It has been previously reported that the level of E-cadherin protein at sites of cell-cell adhesion regulates cadherin adhesiveness (23), therefore we hypothesized that increased E-cadherin expression at these sites may inhibit cell movement by increasing cell-cell adhesion strength. To determine the effect of E-cadherin expression on cell-cell adhesion strength we treated confluent cultures with dispase which results in detachment of the cells in an intact monolayer. The resistance to disaggregation induced by mechanical stress of these monolayers is then used as a measure of the relative strength of cell-cell contacts. Over-expression of E-cadherin resulted in a reduction in the number of single cells detached from the cell sheets, while inhibition of E-cadherin expression by siRNA decreased adhesion strength (Figure 4A), indicating a crucial role for E-cadherin in A431 cell-cell adhesion strength. Treatment of cells with PF-562,271 or knock-down of FAK by siRNA was also observed to increase cell-cell adhesion strength (Figure 4A). Furthermore, inhibition of Src kinase activity by dasatinib increased cell-cell adhesion strength (Figure 4A). However, this was not mediated by increased expression of E-cadherin in the inhibitor treated cells (Figure S6).

To explore the signalling events taking place upon β1-integrin inhibition, we looked at activation of both FAK and Src in β1-integrin siRNA expressing cells. Using vinculin as a marker of integrin adhesions, activation of both Src and FAK in control cells was detected in integrin adhesions (Figure S4D). However, in cells lacking β1-integrin, although FAK was active at integrin adhesions (as measured by pY397 FAK), active Src was absent and furthermore there was no detectable pY861 FAK (Figure S4D). Thus cells lacking β1-integrin are still able to assemble cell-matrix adhesions which contain active FAK. This may be due to incomplete knock down of β1-integrin in the cells or signalling to Y397 FAK from other β-integrin sub-units (16). However, active Src was absent from these adhesions and therefore unable to phosphorylate FAK. Disruption of β1-integrin signalling therefore specifically prevents activation of Src at integrin adhesion sites. In contrast, active Src was still present at integrin adhesion sites in FAK knock down cells (Figure S4E), while the amount of activated Src bound to FAK in wild type cells was decreased in the presence of PF-562,271, as detected by immunoprecipitation (Figure S4F). Thus molecular characterisation of signalling through Src and FAK in both FAK and β1-integrin knockdown cells highlighted a single common event: suppression of Src-dependent phosphorylation of FAK at integrin adhesions (either mediated via loss of activated Src from integrin adhesions (as seen in β1-integrin knockdown cells) or its inability to bind to FAK either through loss of FAK protein (as seen in FAK knockdown cells) or kinase inhibition (PF-562,271 treated

cells)). Taken together with the ability of dasatinib to prevent phosphorylation of FAK on Y861, this suggests that the observed effects on E-cadherin and adhesion strength may be mediated via the Src-dependent phosphorylation of FAK.

To confirm that the ability of Src and FAK to regulate E-cadherin-dependent AJs required the Src-dependent phosphorylation of FAK downstream of β1-integrin signaling we expressed a constitutively active Src mutant (Y527F Src) in A431 cells. Western blotting showed that activated Src and pY861 FAK were increased in cells expressing Y527F Src (Figure S4G). Constitutive activation of Src resulted in a weakening of cell-cell adhesions as measured by an increase in single cells following mechanical disruption (Figure 4B) without causing complete dissolution of cell-cell junctions (Figure S4H). Treatment with a β1-integrin blocking antibody decreased the number of single cells in control cultures but had no effect in cells expressing activated Src (Figure 4B). Thus strengthening of cell-cell junctions following inhibition of β1-integrin is prevented when Src is constitutively active indicating that expression of an un-regulated active Src negates the ability of β1-integrin to control adhesion strength. Furthermore, treatment of cells with dasatinib prevented phosphorylation of FAK on Y861 and increased adhesion strength (Figure 1B and 4A) indicating that Src-dependent phosphorylation of FAK downstream of β1-integrin regulates adhesion strength.

As treatment with PF-562,271 or dasatinib did not alter total E-cadherin protein levels (Figure S6) Src/FAK signaling must regulate E-cadherin function by other mechanisms. E-cadherin-mediated cell-cell junctions are highly dynamic structures and the concentration of E-cadherin specifically at cell-cell junctions is controlled by endocytosis which in turn regulates adhesion strength. To measure endocytosis we followed the internalization of biotinylated cell surface E-cadherin: biotinylated cell surface E-cadherin was progressively enriched in the intracellular pool in control cells while in cells treated with dynasore, a potent dynamin inhibitor that blocks vesicles pinching off the membrane (24), there was no internalization of E-cadherin (Figure 4C). E-cadherin internalization was reduced in β1-integrin siRNA cells (Figure 4C). A similar reduction in E-cadherin internalization was seen in cells treated with dasatinib or when FAK expression was knocked down (Figure 4C).

In support of a link between E-cadherin internalization and adhesion strength, treatment of cells with dynasore also increased adhesion strength (Figure 4A). Furthermore, FRAP analysis of dynasore treated cells showed a reduction in the $t_{1/2}$ of GFP-E-cadherin as was seen following inhibition of Src/FAK signaling (Figure 4D). Thus although measurement of E-cadherin-mediated cell-cell adhesion strength and E-cadherin internalization is not possible *in vivo*, changes in the $t_{1/2}$ may represent an indirect read-out of E-cadherin function that can be measured *in vivo*.

Discussion

We have identified a novel role for Src and FAK in regulating E-cadherin function which is required for the collective movement of tumor cells. In human tumors loss of E-cadherin is associated with more aggressive and invasive tumors. However, it is now evident that the collective movement of tumors, which is dependent on the maintenance of cell-cell junctions, also plays a key role in the invasive capacity of tumors (6). A tight balance exists between E-cadherin expression and collective movement and the dynamic regulation of E-cadherin at cell-cell junctions is crucial in determining junction strength which we have previously linked to the migratory capacity of tumor cells *in vitro* (21). Here we demonstrate that Src/FAK signaling downstream of β1-integrin controls E-cadherin internalization and adhesion strength *in vitro*. Functional measurements of E-cadherin mediated cell-cell adhesion strength and E-cadherin internalization are not currently possible *in vivo* and it is

therefore important to utilize techniques such as FRAP to monitor E-cadherin dynamics which can provide an indirect read-out of E-cadherin function which would otherwise not be possible *in vivo*. The ability of small molecule inhibitors of Src and FAK to alter E-cadherin dynamics *in vivo* correlated with their ability to strengthen cell-cell adhesion, inhibit E-cadherin internalization and importantly inhibit the collective movement of A431 cells *in vivo*. Src and FAK can regulate cell invasion *in vitro* through its role in regulating cell migration and matrix metalloproteinase activity at sites of invadopodia (25-29). These findings identify a novel additional mechanism through which β1-integrin signaling via Src dependent phosphorylation of FAK may regulate the collective movement of tumor cells by modulating cell-cell adhesion strength through control of E-cadherin internalization.

Previously the use of skin flaps has been used to monitor the movement of tumor cells *in vivo* but these studies are restricted by the short period of time that migration can be monitored over and the infrequency that individual cells move *in vivo* within these time frames. To overcome these problems we have utilized optical window chambers, which together with recoverable anesthesia, enabled the repeated imaging of animals over several days. In addition, in contrast to skin flaps, observation windows do not require invasive surgery immediately prior to imaging, and therefore preserve the local tumor microenvironment by minimizing the risk of inflammatory response and tissue damage as a consequence of surgery. Furthermore, images acquired using this method displayed improved signal to noise and increased sample stability, when compared to our previously reported use of skin flaps for FRAP (21). A comparison of FRAP data acquired *in vivo* using skin flaps and optical window imaging methods is shown in Figure S5C,D. The resulting FRAP dataset obtained through the observation windows exhibited R^2 values comparable with those only previously possible *in vitro*. To enable the imaging and quantification of tumor cell movement *in vivo* we combined the implantation of observation windows with the specific labeling of tumor cells using the photoswitchable protein Dendra2, in a similar manner to that recently reported by Kedrin and colleagues (22). Photoswitching of Dendra2 from its green to red emitting state permitted long-term monitoring of tumor cell behavior. In addition, use of the nuclear targeted photoactivatable probe $G^{PA}C$ (14) enabled the quantification of nuclear division *in vivo*. Thus the use of photoswitchable and photoactivatable probes, together with recoverable imaging using optical window chambers, can be used to implement robust and reproducible assays for monitoring the movement and proliferation of tumor cells *in vivo* and provide invaluable information regarding drug action which can help to dissect out the mechanism of action of new therapeutics.

Supplementary Material

Refer to Web version on PubMed Central for supplementary material.

Acknowledgments

This work was funded by Cancer Research UK Program Grant C157/A9148

References

1. Thiery JP. Cell adhesion in development: a complex signaling network. Curr Opin Genet Dev. 2003; 13:365–71. [PubMed: 12888009]
2. Nelson WJ. Adaptation of core mechanisms to generate cell polarity. Nature. 2003; 422:766–74. [PubMed: 12700771]
3. Hajra KM, Fearon ER. Cadherin and catenin alterations in human cancer. Genes Chromosomes Cancer. 2002; 34:255–68. [PubMed: 12007186]

4. Nollet F, Berx G, van Roy F. The role of the E-cadherin/catenin adhesion complex in the development and progression of cancer. Mol Cell Biol Res Commun. 1999; 2:77–85. [PubMed: 10542129]
5. Yap AS. The morphogenetic role of cadherin cell adhesion molecules in human cancer: a thematic review. Cancer Invest. 1998; 16:252–61. [PubMed: 9589034]
6. Friedl P, Gilmour D. Collective cell migration in morphogenesis, regeneration and cancer. Nat Rev Mol Cell Biol. 2009; 10:445–57. [PubMed: 19546857]
7. Avizienyte E, Wyke AW, Jones RJ, McLean GW, Westhoff MA, Brunton VG, et al. Src-induced de-regulation of E-cadherin in colon cancer cells requires integrin signalling. Nat Cell Biol. 2002; 4:632–8. [PubMed: 12134161]
8. Playford MP, Vadali K, Cai X, Burridge K, Schaller MD. Focal adhesion kinase regulates cell-cell contact formation in epithelial cells via modulation of Rho. Exp Cell Res. 2008; 314:3187–97. [PubMed: 18773890]
9. Chen X, Gumbiner BM. Crosstalk between different adhesion molecules. Curr Opin Cell Biol. 2006; 18:572–8. [PubMed: 16859906]
10. Schlaepfer DD, Mitra SK, Ilic D. Control of motile and invasive cell phenotypes by focal adhesion kinase. Biochim Biophys Acta. 2004; 1692:77–102. [PubMed: 15246681]
11. Brunton VG, Frame MC. Src and focal adhesion kinase as therapeutic targets in cancer. Curr Opin Pharmacol. 2008; 8:427–32. [PubMed: 18625340]
12. Joyce JA, Pollard JW. Microenvironmental regulation of metastasis. Nat Rev Cancer. 2009; 9:239–52. [PubMed: 19279573]
13. Miranda KC, Khromykh T, Christy P, Le TL, Gottardi CJ, Yap AS, et al. A dileucine motif targets E-cadherin to the basolateral cell surface in Madin-Darby canine kidney and LLC-PK1 epithelial cells. J Biol Chem. 2001; 276:22565–72. [PubMed: 11312273]
14. Welman A, Serrels A, Brunton VG, Ditzel M, Frame MC. A two color photoactivatable probe for selective tracking of proteins and cells. J Biol Chem.
15. Sandilands E, Cans C, Fincham VJ, Brunton VG, Mellor H, Prendergast GC, et al. RhoB and actin polymerization coordinate Src activation with endosome-mediated delivery to the membrane. Dev Cell. 2004; 7:855–69. [PubMed: 15572128]
16. Brockbank EC, Bridges J, Marshall CJ, Sahai E. Integrin beta1 is required for the invasive behaviour but not proliferation of squamous cell carcinoma cells in vivo. Br J Cancer. 2005; 92:102–12. [PubMed: 15597106]
17. Akiyama SK, Yamada SS, Chen WT, Yamada KM. Analysis of fibronectin receptor function with monoclonal antibodies: roles in cell adhesion, migration, matrix assembly, and cytoskeletal organization. J Cell Biol. 1989; 109:863–75. [PubMed: 2527241]
18. Canel M, Serrels A, Anderson KI, Frame MC, Brunton VG. Use of photoactivation and photobleaching to monitor the dynamic regulation of E-cadherin at the plasma membrane. Cell Adh Migr. 2010; 4
19. Makale M. Intravital imaging and cell invasion. Methods in enzymology. 2007; 426:375–401. [PubMed: 17697892]
20. Macpherson IR, Hooper S, Serrels A, McGarry L, Ozanne BW, Harrington K, et al. p120-catenin is required for the collective invasion of squamous cell carcinoma cells via a phosphorylation-independent mechanism. Oncogene. 2007; 26:5214–28. [PubMed: 17334396]
21. Serrels A, Timpson P, Canel M, Schwarz JP, Carragher NO, Frame MC, et al. Real-time study of E-cadherin and membrane dynamics in living animals: implications for disease modeling and drug development. Cancer Res. 2009; 69:2714–9. [PubMed: 19318551]
22. Kedrin D, Gligorijevic B, Wyckoff J, Verkhusha VV, Condeelis J, Segall JE, et al. Intravital imaging of metastatic behavior through a mammary imaging window. Nature methods. 2008; 5:1019–21. [PubMed: 18997781]
23. Yap AS, Brieher WM, Pruschy M, Gumbiner BM. Lateral clustering of the adhesive ectodomain: a fundamental determinant of cadherin function. Curr Biol. 1997; 7:308–15. [PubMed: 9133345]
24. Macia E, Ehrlich M, Massol R, Boucrot E, Brunner C, Kirchhausen T. Dynasore, a cell-permeable inhibitor of dynamin. Dev Cell. 2006; 10:839–50. [PubMed: 16740485]

25. Zhang Y, Thant AA, Hiraiwa Y, Naito Y, Sein TT, Sohara Y, et al. A role for focal adhesion kinase in hyluronan-dependent MMP-2 secretion in a human small-cell lung carcinoma cell line, QG90. Biochemical and biophysical research communications. 2002; 290:1123–7. [PubMed: 11798192]

26. Hsia DA, Mitra SK, Hauck CR, Streblow DN, Nelson JA, Ilic D, et al. Differential regulation of cell motility and invasion by FAK. J Cell Biol. 2003; 160:753–67. [PubMed: 12615911]

27. Hauck CR, Hsia DA, Puente XS, Cheresh DA, Schlaepfer DD. FRNK blocks v-Src-stimulated invasion and experimental metastases without effects on cell motility or growth. The EMBO journal. 2002; 21:6289–302. [PubMed: 12456636]

28. Hauck CR, Hsia DA, Ilic D, Schlaepfer DD. v-Src SH3-enhanced interaction with focal adhesion kinase at beta 1 integrin-containing invadopodia promotes cell invasion. J Biol Chem. 2002; 277:12487–90. [PubMed: 11839732]

29. Canel M, Secades P, Garzon-Arango M, Allonca E, Suarez C, Serrels A, et al. Involvement of focal adhesion kinase in cellular invasion of head and neck squamous cell carcinomas via regulation of MMP-2 expression. Br J Cancer. 2008; 98:1274–84. [PubMed: 18349846]

Europe PMC Funders Author Manuscripts

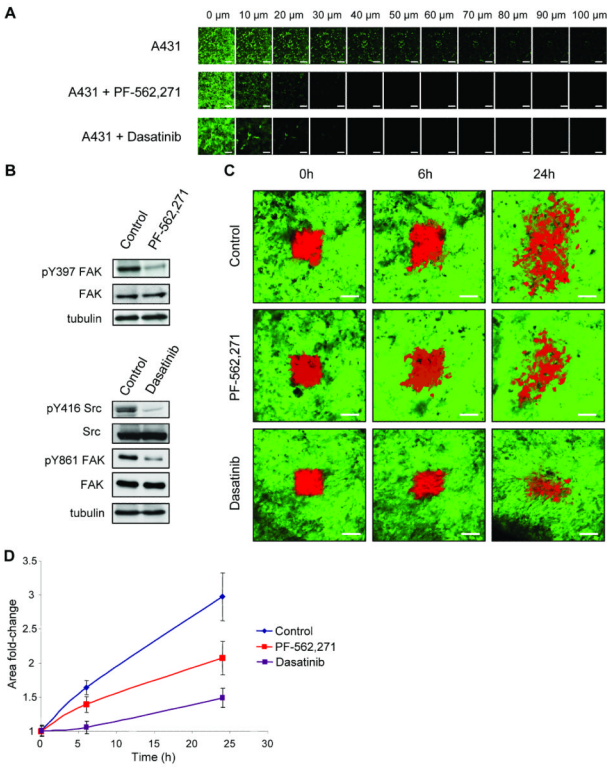

Figure 1.

PF-562,271 and dasatinib inhibit collective cell movement *in vitro* and *in vivo*. (**A**) Invasion of A431 cells into collagen gels in the presence or absence of PF-562,271 or dasatinib. After 5 days, cells were labeled with calcein AM and visualized at 10 μm intervals. The experiment was performed in triplicate and representative series of z-sections at indicated depths through the gel are shown. Scale bars: 200 μm. (**B**) Immunoblot analysis of pY397 FAK and FAK expression in control and PF-562,271 treated cells and pY416 Src, Src, pY861 FAK and FAK in control and dasatinib treated cells. (**C**) Images showing A431 Dendra2 control expressing cells in tumors of untreated mice or mice treated with PF-562,271 or dasatinib, at different time points after photoswitching (red). Scale bars: 100 μm. (**D**) Quantification of the area covered by red fluorescence at shown time points. Values are the mean from at least 5 independent experiments. Error bars: s.e.m.

Europe PMC Funders Author Manuscripts

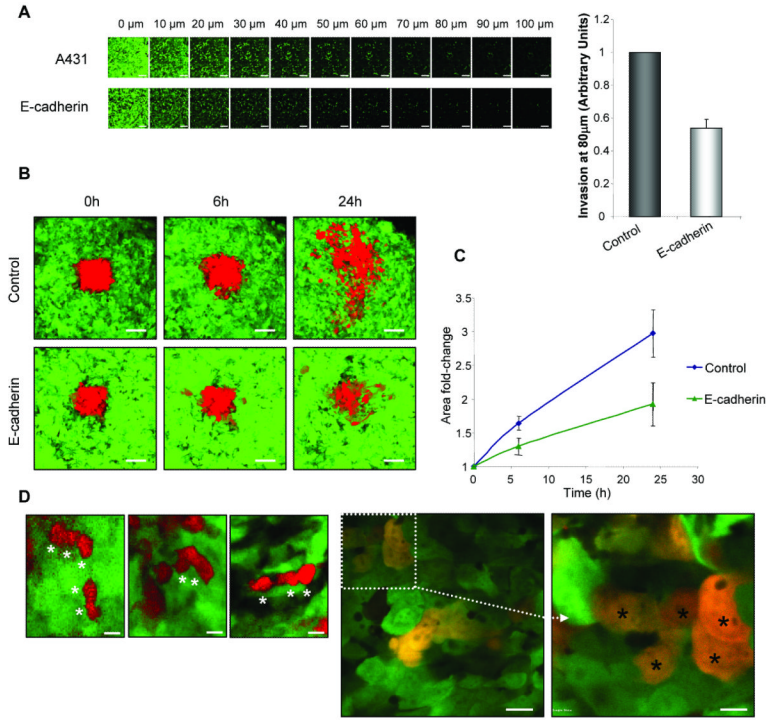

Figure 2.

E-cadherin modulates collective cell movement *in vitro* and *in vivo*. (**A**) Invasion of A431 and A431 GFP-E-cadherin cells into collagen gels. After 5 days, cells were labeled with calcein AM and visualized at 10 μm intervals. Representative series of z-sections at indicated depths through the gel are shown. Scale bars: 200 μm. Quantification of invasion at 80 μm is shown for a representative experiment in a series of three. Values are the mean from triplicate wells. (**B**) Images showing A431 Dendra2 control or GFP-E-cadherin expressing cells in tumors at different time points after photoswitching (red). Scale bars: 100 μm. (**C**) Quantification of the area covered by red fluorescence at shown time points. Values are the mean from at least 5 independent experiments. (**A, C**) Error bars: s.e.m. (**D**) Zoomed images from (**B**) (left panel) and higher magnification images (centre and right panels) showing collective cell movement where individual cells within a group are marked by (*). Scale bars: 20 μm (left and centre images), 10 μm (right image).

Europe PMC Funders Author Manuscripts

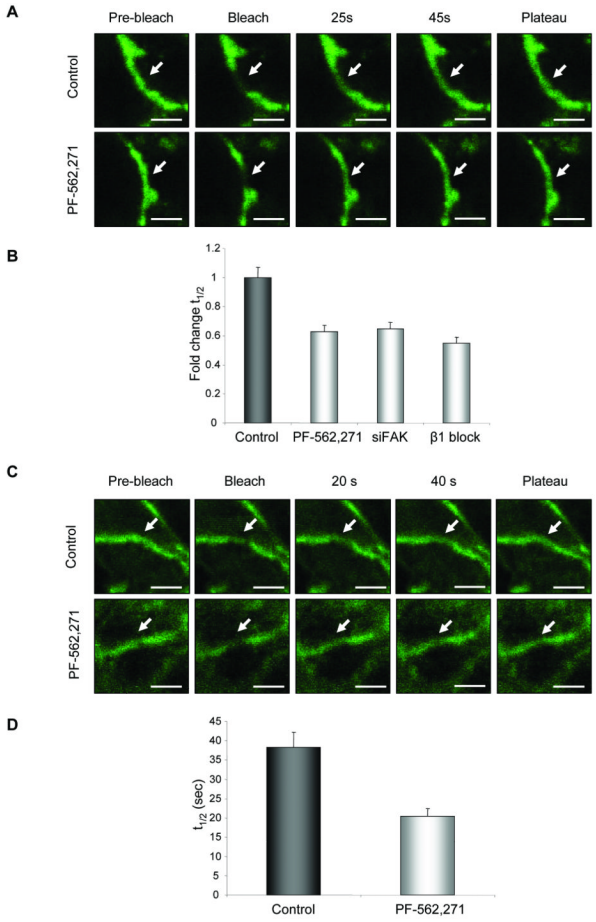

Figure 3.

PF-562,271 alters E-cadherin dynamics *in vitro* and *in vivo*. (**A**) Still images of GFP-E-cadherin at cell-cell junctions in cells untreated (top panels) or treated with PF-562,271 (bottom panels) captured pre-bleach and following bleach. Scale bar: 5 μm. Arrows indicate bleached area (**B**) $t_{1/2}$ of GFP-E-cadherin in control cells or cells treated with PF-562,271, FAK siRNA or β1-integrin blocking antibody. (**C**) Still images of GFP-E-cadherin at cell-cell junctions in tumors untreated (top panels) or treated with PF-562,271 (bottom panels) captured pre-bleach and following bleach. Arrows indicate bleached areas (**D**) $t_{1/2}$ of GFP-E-cadherin in tumors from control or PF-562,271 treated mice. (**A, C**) Scale bars: 5 μm. (**B, D**) Values are the mean from at least 25 cells. Error bars: s.e.m.

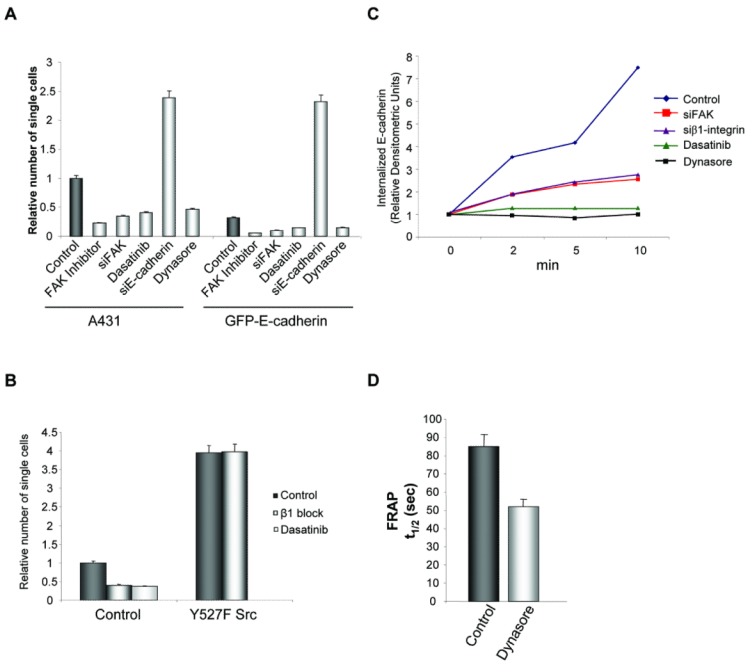

Figure 4.

Inhibition of Src-dependent phosphorylation of FAK downstream of β1-integrin disrupts E-cadherin endocytosis and strengthens cell-cell junctions. (**A**) Number of single cells that disaggregate from a dispase treated monolayer. Values represent the mean from at least three independent experiments. (**B**) Number of single cells that disaggregate from a dispase treated monolayer in control and Y527F Src expressing cells in the presence or absence of β1-integrin blocking antibody or dasatinib. Values represent the mean from at least three independent experiments. (**C**) Quantification of biotinylated E-cadherin internalization over 10 min in control or FAK siRNA cells, β1-integrin siRNA cells, control cells treated with dasatinib or dynasore. (**D**) $t_{1/2}$ of GFP-E-cadherin in control or dynasore treated cells. Values are the mean from at least 25 cells. (**A, B, D**) Error bars: s.e.m.

Europe PMC Funders Author Manuscripts